A coupled chaotic system with different time scales: Toward the implication of observation with dynamical systems

H. Okuda and I. Tsuda

Series ♯230. February 1994

HOKKAIDO UNIVERSITY

PREPRINT SERIES IN MATHEMATICS

♯ 200: S. Izumiya, Y. Kurokawa, Holonomic systems of Clairaut type, 17 pages. 1993.

♯ 201: K.-S. Saito, Y. Watatani, Subdiagonal algebras for subfactors, 7 pages. 1993.

♯ 202: K. Iwata, On Markov properties of Gaussian generalized random fields, 7 pages. 1993.

♯ 203: A. Arai, Characterization of anticommutativity of self-adjoint operators in connection with Clifford algebra and applications, 13 pages. 1993.

♯ 204: J. Wierzbicki, An estimation of the depth from an intermediate subfactor, 7 pages. 1993.

♯ 205: N. Honda, Vanishing theorem for the tempered distributions, 11 pages. 1993.

♯ 206: T. Hibi, Betti number sequences of simplicial complexes, Cohen-Macaulay types and Möbius functions of partially ordered sets, and related topics, 25 pages. 1993.

♯ 207: A. Inoue, Regularly varying correlations, 23 pages. 1993.

♯ 208: S. Izumiya, B. Li, Overdetermined systems of first order partial differential equations with singular solution, 9 pages. 1993.

♯ 209: T. Hibi, Hochster's formula on Betti numbers and Buchsbaum complexes, 7 pages. 1993.

♯ 210: T. Hibi, Star-shaped complexes and Ehrhart polynomials, 5 pages. 1993.

♯ 211: S. Izumiya, G. T. Kossioris, Geometric singularities for solutions of single conservation laws, 28 pages. 1993.

♯ 212: A. Arai, On self-adjointness of Dirac operators in Boson-Fermion Fock spaces, 43 pages. 1993.

♯ 213: K. Sugano, Note on non-commutative local field, 3 pages. 1993.

♯ 214: A. Hoshiga, Blow-up of the radial solitions to the equations of vibrating membrane, 28 pages. 1993.

♯ 215: A. Arai, Scaling limit of anticommuting self-adjoint operators and nonrelativistic limit of Dirac operators, 35 pages. 1993.

♯ 216: Y. Giga, N. Mizoguchi, Existence of periodic solutions for equations of evolving curves, 45 pages. 1993.

♯ 217: T. Suwa, Indices holomorphic vector fields relative to invariant curves, 10 pages. 1993.

♯ 218: S. Izumiya, G. T. Kossioris, Realization theorems of geometric singularities for Hamilton-Jacobi equations, 14 pages. 1993.

♯ 219: Y. Giga, K. Yama-uchi, On instability of evolving hypersurfaces, 14 pages. 1993.

♯ 220: W. Bruns, T. Hibi, Cohen-Macaulay partially ordered sets with pure resolutions, 11 pages. 1993.

♯ 221: S. Jimbo, Y. Morita, Ginzburg Landau equation and stable solutions in a rotational domain, 32 pages. 1993.

♯ 222: T. Miyake, Y. Maeda, On a property of Fourier coefficients of cusp forms of half-integral weight, 12 pages. 1993.

♯ 223: I. Nakai, Notes on versal deformation of first order PDE and web structure, 34 pages. 1993.

♯ 224: I. Tsuda, Can stochastic renewal of maps be a model for cerebral cortex?, 30 pages. 1993.

♯ 225: H. Kubo, K. Kubota, Asymptotic behaviors of radial solutions to semilinear wave equations in odd space dimensions, 47 pages. 1994.

♯ 226: T. Nakazi, K. Takahashi, Two dimensional representations of uniform algebras, 7 pages. 1994.

♯ 227: N. Hayashi, T. Ozawa, Global, small radially symmetric solutions to nonlinear Schrödinger equations and a gauge transformation, 16 pages. 1994.

♯ 228: S. Izumiya, Characteristic vector fields for first order partial differential equations, 9 pages. 1994.

♯ 229: K. Tsutaya, Lower bounds for the life span of solutions of semilinear wave equations with data of non compact support, 14 pages. 1994.

A coupled chaotic system with different time scales: Toward the implication of observation with dynamical systems[#]

H.OKUDA AND I.TSUDA*[†]

Computer Science Center, Nagasaki Institute of Applied Science
Nagasaki, Nagasaki 851-01, Japan
*Department of Mathematics, Faculty of Science, Hokkaido University,
Sapporo, 060, Japan

Abstract

We present three curious phenomena in coupled chaotic systems with different time scales: a copy, an itinerant motion, and 'firework'. The phenomena obtained may provide possible implication of interacting two macroscopic systems, namely 'observing' and 'observed' systems.

[#] A part of this work was done in Kyushu Institute of Technology.
[†] Leaving Kyushu Institute of Technology, Dept. of Artificial Intelligence.

§ 1 Introduction

In this paper, we deal with a coupled chaotic system with different time-scales, motivated chaos-based observation. The system is constituted by two chaotic dynamical systems. To introduce a distinct time-scale in each system explicitly, we couple a two-dimensional map with the discretized equations by Runge-Kutta algorithm of differential equations with three variables, where the evolution time corresponding to one step of Runge-Kutta algorithm is viewed as one discrete time-step of the map. In this coupled system, we found various kinds of behaviors.

A coupled chaotic system has been well studied, motivated the better understanding of turbulence(for instance, K.Kaneko, 1992; R. J. Deissler, 1987), complex electric circuits like nerves(V. Perez-Munuzuri, V. Perez-Villar and L. O. Chua, 1992), spatial nonlinear dynamics(J. P. Crutchfield and K. Kaneko, 1987), and even motivated various interesting features of itself as complex systems(for instance, K. Kaneko, 1990; I. Waller and R. Kapral, 1984). If one is concerned with complex dynamics like one in brain, however, the studies in this area so far may not be sufficient. One point lacked is a description of coupled systems with distinct time-scales.

The introduction of distinct time-scales in this paper is unusual. Since we use Runge-Kutta discretization, the reader might be concerned with spurious solutions that could be obtained by discretizing ODEs. Actually, spurious solutions were found in Euler's discretization(M. Yamaguchi and H. Matano, 1979; H. -O. Peitgen, M. Prufer and K. Schmitt, 1988). This situation can occur also in Runge-Kutta discretization. However, it was also proved that Runge-Kutta discretization is robust for getting real solutions if evolution time is sufficiently small. We here chose an appropriate evolution time to avoid spurious solutions that are qualitatively far from real solutions.

In section 2 , we report an itinerant motion and a copy found in uni-directionally coupled system. In section 3, we characterize these behaviors by means of the Lyapunov spectrum and the information flow. We also atempt to show the mechanism. In section 4, we report another type of behavior found in bi-directionally coupled system, which is called 'firework' that appears as a quite different attractor in size from the ones in the isolated systems. Section 5 is devoted to concluding remarks.

§ 2 Dynamics of uni-directionally coupled system

In this section, we show a dynamic behavior in uni-directionally coupled system. The model is expressed as follows:

$$\begin{aligned} x(n+1) &= F(x(n)) + Cf(v), \\ dv/dt &= G(v), \end{aligned} \tag{1}$$

where $x \in \mathbf{R}^k, v \in \mathbf{R}^m, n$ a discrete time, t a continuous time, and f is, in general, a nonlinear function of components of v, but here we study the case of a linear coupling. Furthermore, F and G are nonlinear.

In the simulation of eq.(1), we used the Runge-Kutta algorithm, whereby the

equation (1) is reformulated by eq.(2) in computation.

$$x(n+1) = F(x(n)) + Cf(v(n)), \qquad (2)$$
$$v(n+1) = v(n) + \Delta G(v(n)),$$

where ΔG is an increment of G in the Runge-Kutta algorithm, which is assumed small.

In case of the inverse coupling from map to continuous system, the overall behavior could be a Brownian motion, triggerd by a 'random' force if F is a fully chaotic map. Whereas, we now consider the forced system by a slowly varing variables, since we are concerned with how and to what extent the semi-macroscopic (dissipative but close to conservative system with fast variables) 'observer' receives the information of the dissipated macroscopic world. In the present paper, we investigate mainly a sine-map forced by the Lorenz system.

$$\begin{aligned} x_1(n+1) &= \sin(ax_1(n) + bx_2(n)) + Cv_1(n), \\ x_2(n+1) &= \sin(cx_1(n) + dx_2(n)) + Cv_3(n), \\ v_1(n+1) &= v_1(n) + \Delta K(v_1(n), v_2(n), v_3(n)), \\ v_2(n+1) &= v_2(n) + \Delta L(v_1(n), v_2(n), v_3(n)), \\ v_3(n+1) &= v_3(n) + \Delta M(v_1(n), v_2(n), v_3(n)), \end{aligned} \qquad (3)$$

where $\Delta K, \Delta L, \Delta M$ are increments in the Runge-Kutta discretization of the Lorenz system. The Lorenz system is given as follows(Lorenz, 1963):

$$\begin{aligned} dv_1/dt &= -\sigma v_1 + \sigma v_2, \\ dv_2/dt &= -v_2 + rv_1 - v_1 v_3, \\ dv_3/dt &= -\beta v_3 + v_1 v_2, \end{aligned} \qquad (4)$$

We choose the parameters of the sine-map a, b, c and d such that the isolated sine-map has only periodic points as an attractor, and we also choose a small value of the coupling constant. Then we found copies of the Lorenz attractor around the periodic points in $x_1 - x_2$ plane of the sine-map(Fig.1(a),(b)). One can easily control the number of the copy, selecting the period in the isolated sine-map: n-periodic points for n copies. One may also control the size of copied attractor, tuning the value of the coupling constant in its appropriate range.

-Fig.1(a)-
-Fig.1(b)-

This kind of copy can also be obtained, using an intermittent chaos. We set up the parameter values of the sine-map to exhibit intermittent chaos after coupling. The overall trajectory is shown in Fig.2. A magnification in the neighborhood of each destabilized periodic point through the saddle-node bifurcation shows a slightly distorted Lorenz attractor and fine unstable manifold connecting the Lorenz attractor with the other chaotic region(see Fig.3).

-Fig.2-

-Fig.3(a)-
-Fig.3(b)-

In such a case a long stay, in the neighborhood of the unstable periodic points, due to the appearance of intermittency is essential for the copy. In this period, the slow variables affect the fast variable almost linearly. The orbit stays for a long time on the distorted quasi-attractor (with the form of the Lorenz attractor without Cantor set) and begins to escape from such an attractor when orbit reaches to the edge of the chaotic region. A time series of the variable x_1 depicted in the lower part of Fig.2 clearly shows the intermittency. When the size of the copied attractor is allowed to become large with the increase of distortion, we obtain itinerant motion between two chaotic regions. One example is shown in Fig.4(a). A coupling constant C is larger than the one in the copy process. An itinerant motion beween two chaotic clusters is seen. These clusters are considered 'quasi-attractors'. A fine manifold connecting the clusters is a ruin of the Lorenz attractor(a partial copy of the Lorenz attractor excepting Cantor set). The time series of variable x_1 is shown in Fig.4(b). The schematic drawing of the feature is shown in Fig.5, where two quasi-attractors denoted by ② and ④ are connected by the fine channels of manifold, ①, ③, ⑤,and ⑥ in order of $(① \to ③)^n \to (⑤ \to ⑥)^m$, where $(k \to \ell)^n$ means n-fold of the sequence $(k \to \ell)$.

-Fig.4(a),(b)-
-Fig.5-

It is still questionable whether or not the itinerant motion obtained here is equivalent to chaotic itinerancy(K. Ikeda, K. Otsuka and K. Matsumoto, 1989; K. Kaneko, 1990; P. Davis, 1990; I. Tsuda, 1992). The notion of chaotic itinerancy has been proposed by the above authors with unanimous cooperation in order to elucidate a dynamic behavior with a long history. Chaotic itinerancy has been observed in high dimensional dynamical systems. In the present case, in place of high dimension, a distinct time-scale was introduced, whereby a similar behavior to chaotic itinerancy was observed.

§ 3 Characterization and mechanism of the dynamics

In this section, we investigate a dynamic feature of the behaviors in terms of several quantities, whereby the mechanism can be elucidated.

3-1 *The Lyapunov spectrum*

The Lyapunov spectrum are calculated by the conventional method of Shimada and Nagashima(1978). Figure 6 shows the Lyapunov spectrum of the attractor shown in Fig.4. The spectrum is $(+,+,-,-,-)$, hence practically the system exhibits chaos. The computed result is the following: $(9.94\times10^{-4}\pm3.75\times10^{-6}, 1.38\times10^{-4}\pm4.1\times10^{-6}, -1.61\times10^{-2}\pm2.15\times10^{-6}, -0.17\pm9.42\times10^{-4}, -0.24\pm1.84\times10^{-4})$. The Lyapunov dimension (J. L. Kaplan and J. A. Yorke, 1979) in this case can be estimated as dim Λ=2.062. The largest exponent apparently stems from the positive exponent of the Lorenz system. The positiveness, though small, of the second exponent is questionable. It may be a numerical problem in a system with distinct time scale. The attractor in Fig.4(a) in $x_1 - x_2$ plane is constructed by just one orbit. Indeed, different initial conditions converge to one trajectory after transient motion. A seemingly chaotic motion depends on the long past history, so that we call it an itinerant motion.

-Fig.6-

3-2 *Time-dependent mutual information*

It would be valuable to study what kind of informational structure is constructed in the process of the dynamics. To see this, we calculated time-dependent mutual information between the sine-map and the Lorenz system. In determination of a state, we chose only one variable in each system, say x_1 and v_1. Since the coupling is uni-directional from the Lorenz system to the sine-map, the mutual information betweem the two systems indicates the information content flowed from the Lorenz system to the sine-map. Defining a time-dependent mutual information as follows(K. Matsumoto and I. Tsuda 1985, 1987, 1988), one can know the information structure of the chaotic itinerant motion.

$$I_{x,v}(t) = -\Sigma_j p(x_j) \log p(x_j) + \Sigma_i \Sigma_j p(v_i) p(x_j/v_i;t) \log p(x_j/v_i;t), \tag{5}$$

where $p(x_j)$ is a stationary probability of a variable x_1 taking a state j, and $p(x_j/v_i;t)$ a time-dependent conditional probability that x_1 takes a state j at t time-steps after v_1 having taken a state i. This quantity expresses the information content conveyed by the variable v_1 among the information of the variable x_1 possessing.

Figure 7 shows the time-dependent mutual information in the case of intermittent chaos of Fig.2, where 100 states are taken in both variables x_1 and v_1, i.e., $i, j = 0, \cdots 99$.

-Fig.7-

The calculated mutual information is oscillatory, and its envelop shows a power decay in time:

$$I_{x,v}(t) = I_0 t^{-a} \tag{6}$$

where I_0 is an initial information (at t=1). Taking the logarithm of both sides of eq.(6), and replacing the variable $\log t$ by s, eq.(7) follows.

$$\log I_{x,v}(s) = \log I_0 - as, \tag{7}$$

Taking a derivative of both sides with respect to s, we obtain eq.(8).

$$I'_{x,v}(s)/I_{x,v}(s) = -a, \tag{8}$$

where $I'_{x,v}(s) = dI_{x,v}(s)/ds$.
This means that the same ratio of information decays at each time-step in a logarithmic time-scale.

One can also use an algorithm for calculating a bit-wise mutual information(K. Matsumoto and I. Tsuda, 1987), namely, one can calculate information flow between any two binary digits, adopting a binary expansion of a variable. The same ratio of the information decay means that an information mixing takes place in binary space. Thus, each binary digit may contain information of almost every digit. In the present case, the information mixing takes place in binary space with an elongated time scale: the mixing speed becomes slower and slower, accompanied with the dynamics. The advantage of this type of decay of information lies in the system's cability of dynamic storage of information conveyed from another system.

3-3 *Dynamical mechanism of copy and itinerancy*

In this subsection, we inquire a mechanism of the copy and the itinerant motion of the coupled system. Our system can be rewritten as follows.

$$x(n+1) = F(x(n)) + Cf(v(n)) \tag{2'a}$$
$$v(n+1) = v(n) + \Delta t G(v(n)), \qquad \Delta t \ll 1, \tag{2'b}$$

where f has components constituted by the components of v. Since v is a slowly varying variable compared with x, the second term of the right hand side of eq.(2'a) is considered as a constant during a period of, roughly, the order of Δt^{-1}. Thus, eq.(2'a) can be replaced during this period by the following equation (9):

$$x(n+1) = F(x(n)) + k, \tag{9}$$

where k is a constant vector.

Depending on the value of components of k, this dynamics can have three stages of dynamics, each described by one of the following equations.

$$x(n+1) = x(n) + k \tag{10}$$
$$x(n+1) = Ax(n) + k \tag{11}$$
$$x(n+1) = F(x(n)) + k, \tag{12}$$

where A is a non-identical constant matrix.
When the system follows eq.(10), its orbit in space x is described as a trace of a drifting point influenced by the differential system(eg., the Lorenz system), whose point is a fixed point of the isolated map(eg., sine-map). When the coupling constsnt C is relatively small, the copy of the attractor (excepting Cantor set) is achieved in the neighborhood of the fixed point. Whereas, when C is relatively large, only the part of the attractor can be copied. When the system follows eq.(11), the orbit is described as a trace of a drifting spiral motion if a matrix A has at least one pair of complex eigen values. Finally, when the system follows eq.(12), the orbit could be chaotic due to nonlinearity of the map. Taking into account the all stages of dynamics, one may conclude that actual orbits behave as if it is intermittent with a long past history.

In order to check the plausibility of the above scheme, we introduced a 'distance plot'(Tsuda & Okuda, 1994). We define a distsnce plot as to indicate a distribution in a phase space of temporal(or transient) characteristic quantity of dynamical orbits. Several kinds of indications can be taken into account. We will report them in a separate paper in detail(Tsuda and Okuda 1994). Among others, here we present the definition of one kind of distance plot. The distance plot $L^\tau(x_0)$ is defined as a distribution in phase space of the Euclidean distance between corresponding positions of orbit at time t and $t+\tau$, where x_0 is an initial position.

$$L^\tau(x_0) = \|F^t(x_0) - F^{t+\tau}(x_0)\|, \tag{13}$$

where $F^t(x_0)$ is an orbital point at time t of the dynamical system F with initial condition x_0, and $\| \bullet \|$ an Euclidean norm of $\bullet$.

The distribution is plotted in phase space, for instance, in $x_1 - x_2$ plane. Every position in a plane can be classified by colors according to the distance. Here, we plot the distribution of the distance in $k_1 - k_2$ plane in the following system:

$$\begin{aligned} x_1(n+1) &= \sin(ax_1(n) + bx_2(n)) + k_1 \\ x_2(n+1) &= \sin(cx_1(n) + dx_2(n)) + k_2 \end{aligned} \tag{14}$$

where k_1 and k_2 are components of constsant vector k, and τ is fixed to some value. The result is shown in Fig.8. Some orbits of the Lorenz chaos projected on $v_1 - v_3$ plane are superimposed in the distance plot. An overall dynamics is executed synchronously with the Lorenz dynamics(Fig.8(b)). The computed orbit is classified by color corresponding to the position of the Lorenz orbit(Fig.8(a)). The value of τ was determined as the time when the orbit falls into attractor, so that here $\tau = 10$.

-Fig.8(a),(b)-

The overall dynamics copies the Lorenz orbits when the Lorenz orbits locate in the places where the distance keeps small values. When the Lorenz orbits pass through the places of the intermediate value of the distance, the overall dynamics exhibits periodically modulated behaviors. Once the Lorenz orbits arrive at the places of higher values in the distance plot, the orbit starts to behave chaotically. Thus, the orbit identification by distance plot assures the above decomposition, eq.(10)-(12).

§4 Dynamics of bi-directionally coupled system

In this section, we consider the mutually coupled system with explicitly different time scales. The system used is as follows:

$$\begin{aligned} x_1(n+1) &= \sin(ax_1(n) + bx_2(n)) + C_1 v_1(n) \\ x_2(n+1) &= \sin(cx_1(n) + dx_2(n)) + C_1 v_3(n) \\ v_1(n+1) &= v_1(n) + \Delta K(v_1(n), v_2(n), v_3(n)) + C_2 x_1(n) \\ v_2(n+1) &= v_2(n) + \Delta L(v_1(n), v_2(n), v_3(n)) \\ v_3(n+1) &= v_3(n) + \Delta M(v_1(n), v_2(n), v_3(n)) + C_2 x_2(n), \end{aligned} \tag{15}$$

where C_1 and C_2 is a coupling constant. The typical dynamics are shown in Fig.9.

-Fig.9(a)-

-Fig.9(b)-

When the values of both coupling constants are large, the orbit tends to converge to a fixed point or to diverge. However, a curious phenomenon appears in some combination of C_1 and C_2. The orbit stays in the neighborhood of the initial position ($\sim$ (0, 0)) untill the first around 40,000 steps ($t = 0 \sim 4$). At the next stage, the orbit draws a horseshoe and spirals out rather regularly, but after a while it spirals in rather chaotically and shrinks. After that, the orbit begins to move straightly in the positive or the negative direction along the v_1 axis depending on the initial conditions(Fig.10(a)). As soon as the orbit reaches to the place at $v_1 \sim 25{,}000$ or $v_1 \sim -25{,}000$, the orbit explodes and then constructs a huge chaotic attractor as shown in Fig.10(b). This critical region of explosion is very thin that

is almost orthogonal to the v_1 direction. The size of the attractor is about 10^6 times of the one in the isolated system.

-Fig.10(a),(b)-

Figure 11 shows the distance plot on $v_1 = -25,000$, i.e., (v_2, v_3) — plane, which may indicate an existence of the stable manifold of the huge attractor. This manifold is also unstable manifold of the saddle that is generated close to $v_1 = -25,000$ — plane via the bilateral coupling.

-Fig.11-

Figure 12(a) is a schematic drawing of this feature in five-dimensional phase space. We call this dynamical behavior 'firework'. The firework is due to the generation of the heteroclinic orbit connecting saddles. The connection of the two saddles, $S_0(v_1 = 0)$ and $S_1(v_1 = -25,000)$ does not generate intersection of stable and unstable manifold of the saddle S_1, but the other connections among the other saddles locating far from S_0 and S_1 possesses heteroclinic intersection, which gives rise to strange attractor(see also Fig.12(b)). A variable v_3 of the Lorenz system has a value of zero for a long time while v_1 only across a value of zero. Then the positive feedback becomes dominant by the mutual coupling of x_1 and v_1, which drives a variable v_1, but not v_3.

The firework may be in the same class as crisis (C. Grebogi, E. Otto, and J. A. Yorke, 1983) in its geometric features, but it has some new characteristics: the unusual size change of attractor, and a dynamic manifestation of a chain of unstable manifold of different type of attractors.

-Fig.12(a),(b)-

The firework itself is stable for noise, but since the system has many basins of attraction, even infinity, the complex transition among basins by noise can be seen. Actually, when we add the noise to the orbits staying at the huge attractor, the orbit can leave the attractor, then diverges or returns to the neighborhood of the v_3 axis and again moves to another huge attractor (Fig.13).

-Fig.13-

We numerically found a simple relation of C_1 and C_2 which generates firework(Fig.14), that is, $C_1 C_2^a = b$, where $a = -1.2$ and b=0.04. A further investigation is necessary to elucidate this relation.

-Fig.14-

§ 5 Concluding remarks

We presented a new type of coupled chaotic systems, where we found curious behaviors: the copy, itinerant motion, and firework. A characteristics of the dynamics is two distinct time scales which were introduced explicitly. This study is motivated in the exploration of the explicit model system that may simulate the interacting process between the 'observer' and the 'observed system'. The proposed system is simply a combination of simple dynamical syatems, thus it should not be regarded the 'same' system as neural assemblies. Nevertheless, there seems room to expect that the dynamics reported here could be the implication of observation process of cortical neuro-assemblies, since the cortical activities at the level of neuro-assemblies has, probably, much different time-scales from the ones in the outer world.

References

Crutchfield, J. P., Kaneko, K. [1987] "Phenomenology of spatio-temporal chaos," Directions in chaos, 1, 272-353.

Deissler, R. J. [1987] "Spatially growing waves, intermittency, convective chaos in an open-flow system," Physica D, 25, 233-260.

Grebogi, C., Otto, E., Yorke, J. A. [1983] "Crises, sudden changes in chaotic attractors, and transient chaos," Physica D, 7, 181-200.

Kaneko, K. [1990] "Clustering, coding, switching, hierarchical ordering, and control in a network of chaotic elements," Physica D, 41, 137-172.

Kaneko, K. [1992] "Overview of coupled map lattices," Chaos, 2, 279-282.

Kaplan, J. L. & Yorke, J. A. [1979] "Chaotic behavior of multidimensional difference equations," in Functional Differential Equations and Approximation of Fixed Points, eds.

Lorenz, E. N. [1963] "Deterministic non-periodic flow," J. Atmos. Sci. 20, 130-141.

Matsumoto, K. & Tsuda, I. [1985] "Information theoretical approach to noisy dynamics," J. Phys. A18, 3561-3566.

Matsumoto, K. & Tsuda, I. [1987] "Extended information in one-dimensional maps," Physica D26, 347-357.

Matsumoto, K. & Tsuda, I. [1988] "Calculation of information flow rate from mutual information," J. Phys. A21, 1405-1414.

Peitgen, H. -O., Prufer, M., & Schmitt, K. [1988] "Newton flows for real equations," Rocky Mt. J. Math., 18, 433-444.

Perez-Munuzuri, V., Perez-Villar, V., & Chua, L. O. [1992] "Propagation failure in linear arrays of Chua's circuits," Int. J. Bifurcation and Chaos 2, 403-406.

Shimada, I. & Nagashima, T. [1979] "A numerical approach to ergodic problem of dissipative dynamical systems," Prog. Theor. Phys. 61, 1605-1614.

Tsuda, I. & Okuda, H. [1994] in preparation.

Waller, I. & Kapral, R. [1984] "Synchronization and chaos in coupled nonlinear oscillators," Phys. Lett. A105, 163-168.

Figure Captions

Fig.1

A copy of the Lorenz attractor.
The parameter values:$\sigma = 10, r = 35, \beta = 4, a = 0, b = -2.41, c = 1, d = 1.1, C = 0.001, \Delta t = 0.0001$.
(a) The whole attractor projected in phase space $x_1 - x_2$. Six clusters are seen.
(b) A magnification of one of the clusters. The Lorenz attractor(without Cantor set) is seen.

Fig.2

The whole attractor projected in phase space $x_1 - x_2$ in intermittent chaos. A time serise of trajectory of x_1 indicating the intermittent motion is shown in the lower part of the figure.
The parameter values:$\sigma = 10, r = 35, \beta = 4, a = 0, b = -2.677, c = 1, d = 1, C = -0.0001, \Delta t = 0.0001$.

Fig.3

(a) The 44 magnifications of the upper central part of Fig.2. A copy of distorted shape of the Lorenz attractor is seen. All parameter values are the same as in Fig.2.
(b) The 44 magnifications in the x_1 direction and 10 magnifications in the x_2 direction of the upper central part of Fig.2. A copy of the projected Lorenz attractor and the fine unstable manifold connecting the projected Lorenz attractor with the other chaotic region are seen. All parameter values are the same as in Fig.2.

Fig.4

(a) An itinerant motion in $x_1 - x_2$ space.
Parameter values:$\sigma = 10, r = 33, \beta = 4, a = 0, b = -1.5, c = 1, d = 1, \Delta t = 0.0001$.
(b) A time series of the variable x_1. An increment of time evolution is $\Delta t = 0.0001$.

Fig.5

A schematic drawing of an itinerant motion. Numbers in the figure indicate a sequence of trajectory.

Fig.6

An evolution of Lyapunov spectrum of the attractor shown in Fig.4(a).
Black line is a time series of the largest exponent and green, blue, red and violet are the 2nd, 3rd, 4th and 5th exponent respectively.

Fig.7

A time course of mutual information $I_{x,v}(t)$ (log-log plot) between two systems in the case that $\Delta t = 0.005, t = 0 \sim 5, \sigma = 10, r = 35, \beta = 10, a = 0, b = -2.677, c = 1, d = 1$, and $C = -0.0001$(see also Fig.2). The range of phase

space $x_1 = -1.1 \sim 1.1, v_1 = -25 \sim 25$ are divided into 100 partitions for the calculations.

Fig.8

(a) A distance plot in $k_1 - k_2$ plane ($\tau = 10$). A part of the Lorenz chaos($v_1 - v_3$ plane) are superimposed with white curve(up to $t = 0.8$ with an increment $\Delta t = 0.00001$).
(b) A trajectory in $x_1 - x_2$ is drawn synchronously in color with Lorenz dynamics. A correspondence between values of distance and colors is as follows : Code = (Value of distance) $\times$ 4(modulo 7)+1.
Code = 1 $\rightarrow$ dark blue, Code = 2 $\rightarrow$ green, Code = 3 $\rightarrow$ blue, Code = 4 $\rightarrow$ red, Code = 5 $\rightarrow$ violet, Code = 6 $\rightarrow$ yellow, and Code = 7 $\rightarrow$ black.
Parameter values : $\sigma = 10, r = 33, \beta = 4, a = 0, b = -1.5, c = 1, d = 1$, and $C = 0.04$.

Fig.9

Typical dynamics of bi-directionally coupled system with small value of coupling constant.
(a) A trajectory in $v_1 - v_3$ space. (b) A trajectory in $x_1 - x_2$ space.
Parameter values : $\sigma = 10, r = 33, \beta = 4, a = 0, b = -1.5, c = 1, d = 1, C_1 = 0.001, C_2 = 0.3$, and $\Delta t = 0.0001$.

Fig.10

(a) A curious behavior of bi-directionally coupled system (the first 5×10^4 steps are shown). Coupling constants : $C_1 = 0.0008, C_2 = 4.6$. The other parameter values are the same as in Fig.9.
(b) A huge attractor of 'firework' (shown up to $t = 20$). Dots in the neighborhood of the center are the trajectories of the first, around 5×10^4 steps. The other parameter values are the same as in Fig.10(a).

Fig.11

The distance plot in $v_2 - v_3$ plane.
A color coding is as follows : Code = (Value of distance)/100,000 (modulo 7)+1.
Code = 1 $\rightarrow$ dark blue, Code = 2 $\rightarrow$ green, Code = 3 $\rightarrow$ blue, Code = 4 $\rightarrow$ red, Code = 5 $\rightarrow$ violet, Code = 6 $\rightarrow$ yellow, Code = 7 $\rightarrow$ black, and if (Value of distance)/100,000 is greater than 300, then take white. $\Delta t = 0.0001, t = 0.01$.
The other parameter values are the same as in Fig.10.

Fig.12

(a) A schematic drawing of stable and unstable manifold of 'firework' in five-dimensional phase space.
(b) A schematic drawing of heteroclinic intersection.

Fig.13

Orbits of 'firework' after adding the random noise to the variables v_1 and v_3.
Numbers in the figure indicate the sequence of the orbit.
The amplitude of the random noise is 50.
$C_1 = 0.028, C_2 = 0.05$. The other parameter values are the same as in Fig.9.

Fig.14

The relation of C_1 and C_2 that generates 'firework' (log – log plot).

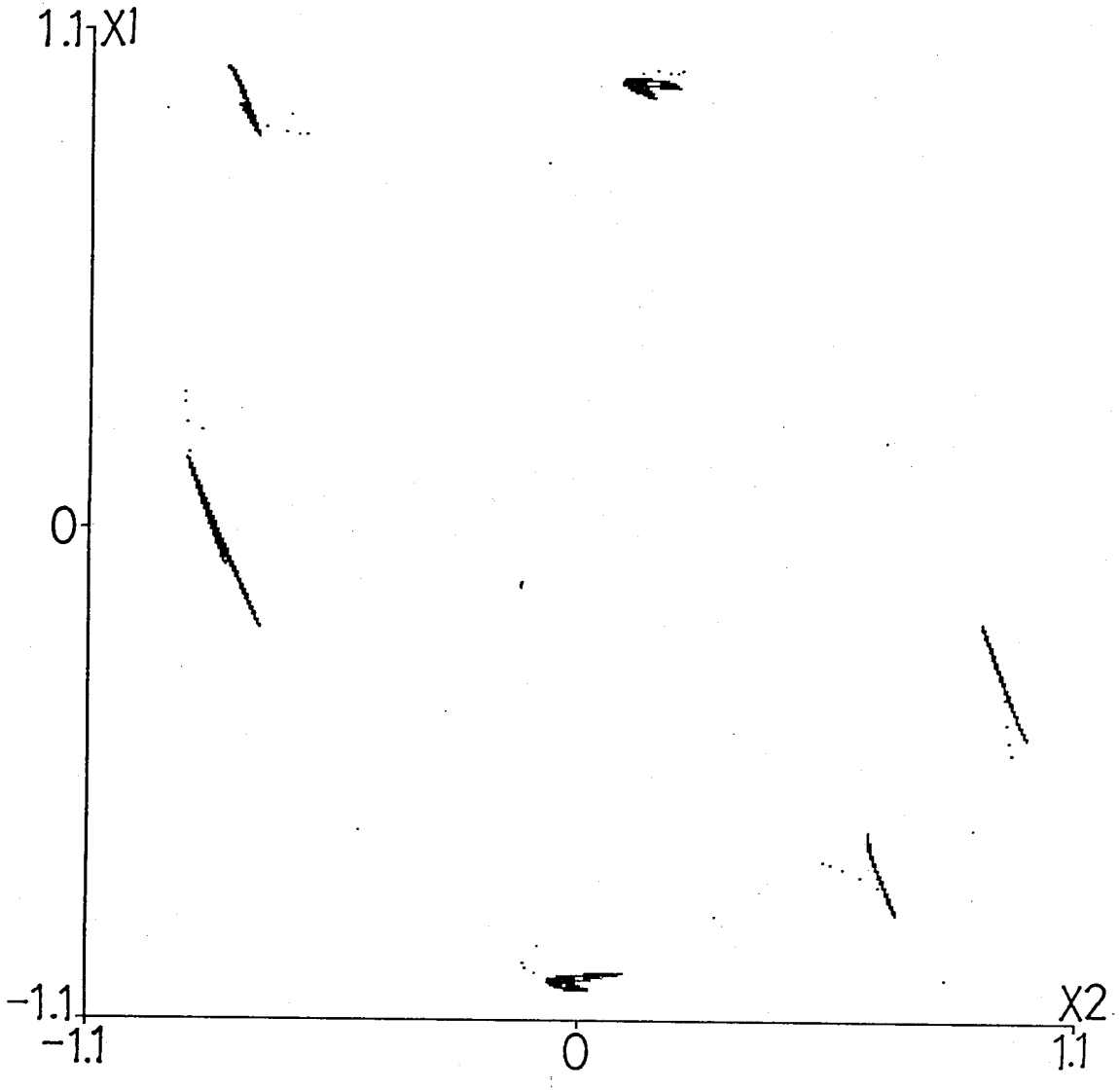

Okuda & Tsuda

Fig. 1 (a)

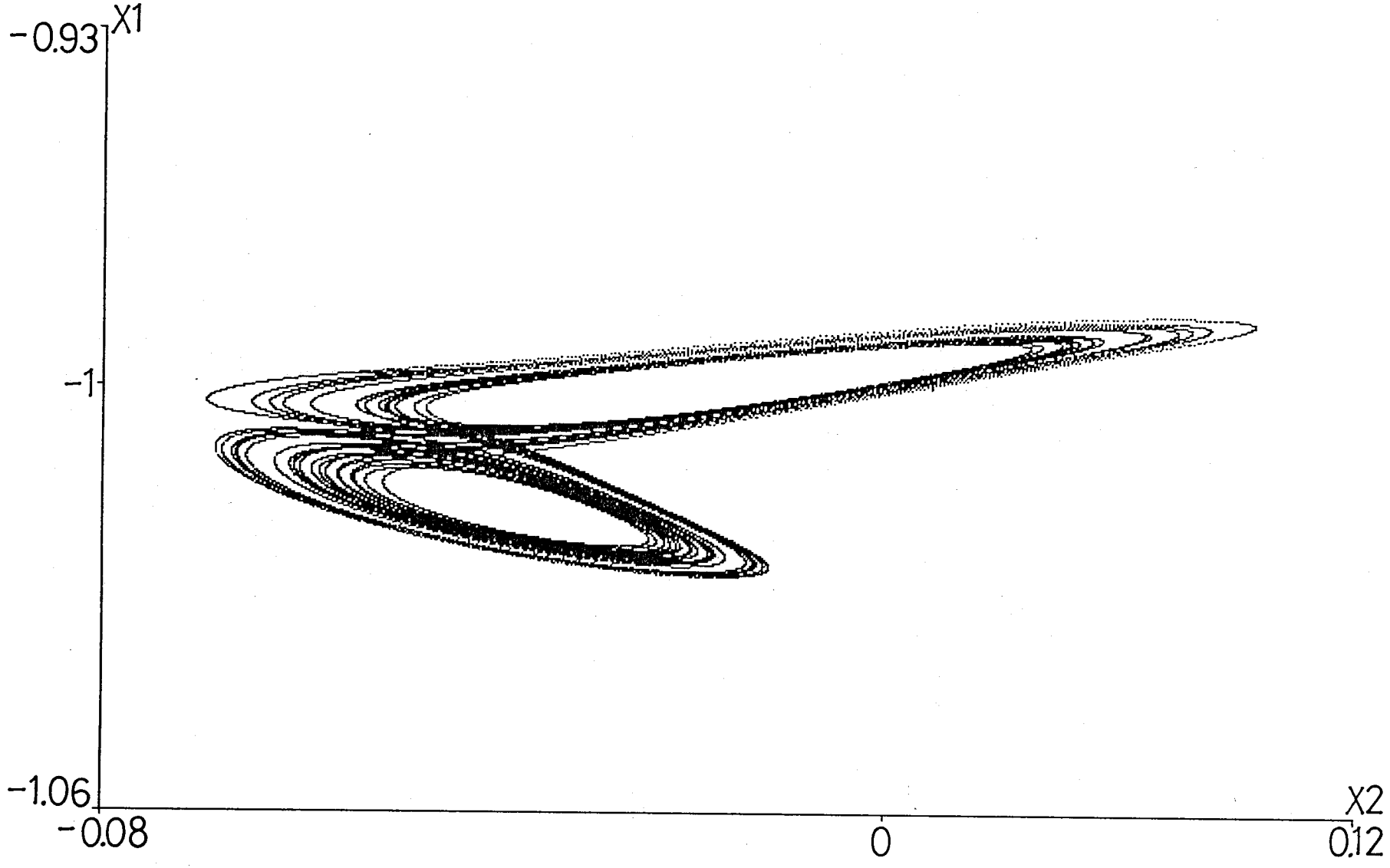

Okuda & Tsuda

Fig 1. (b)

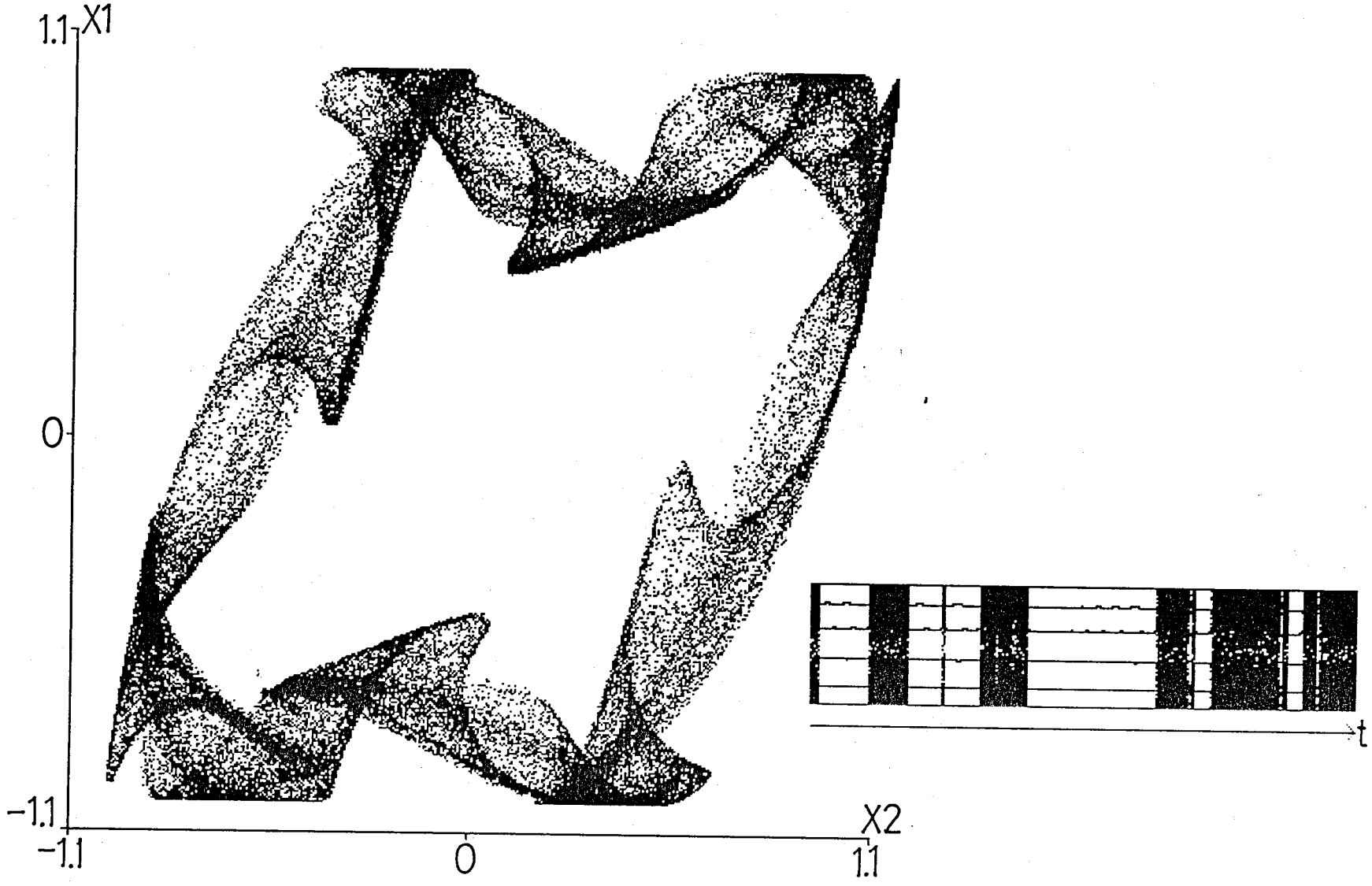

Fig. 2 Okuda & Tsuda

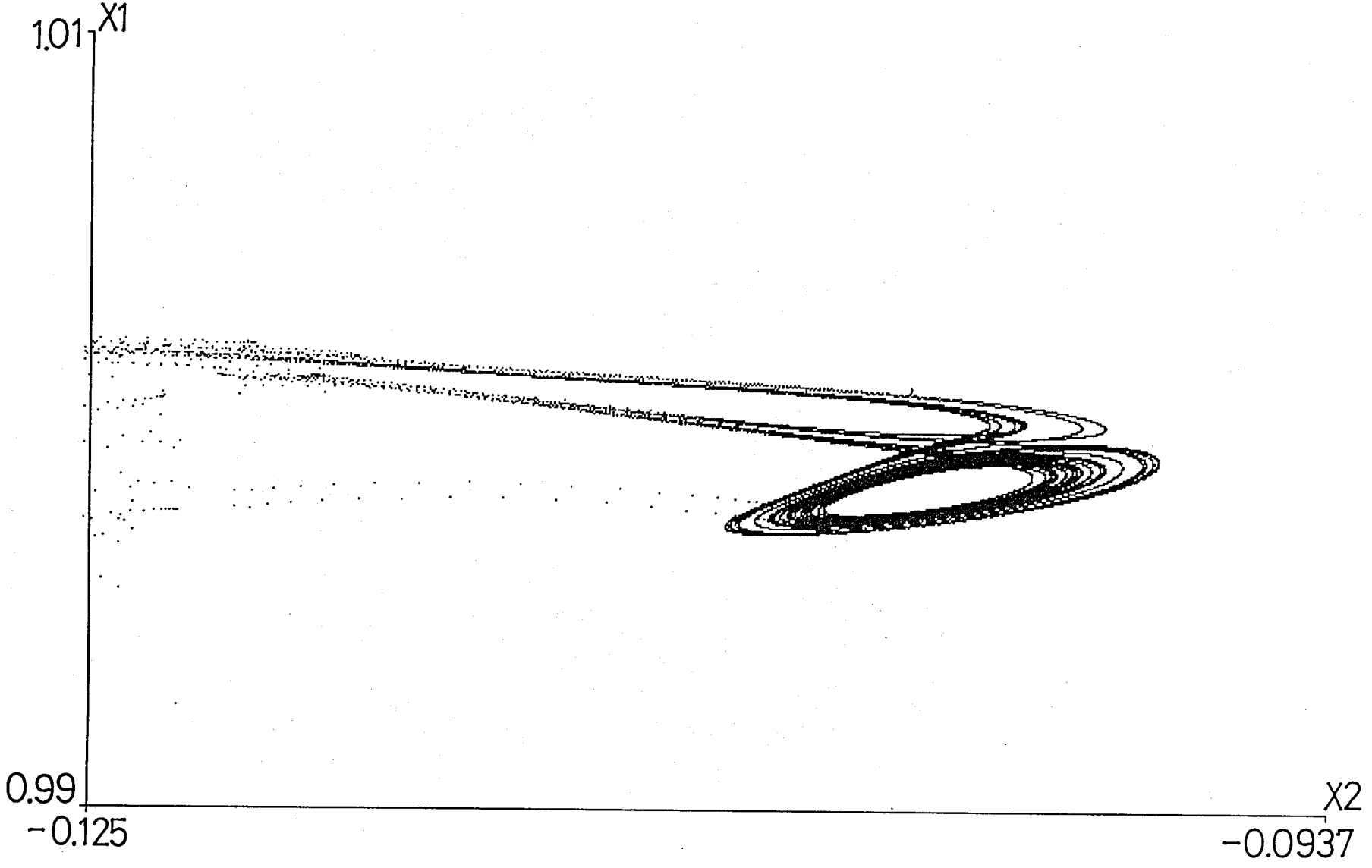

Fig 3 (a)

Okuda & Tsuda

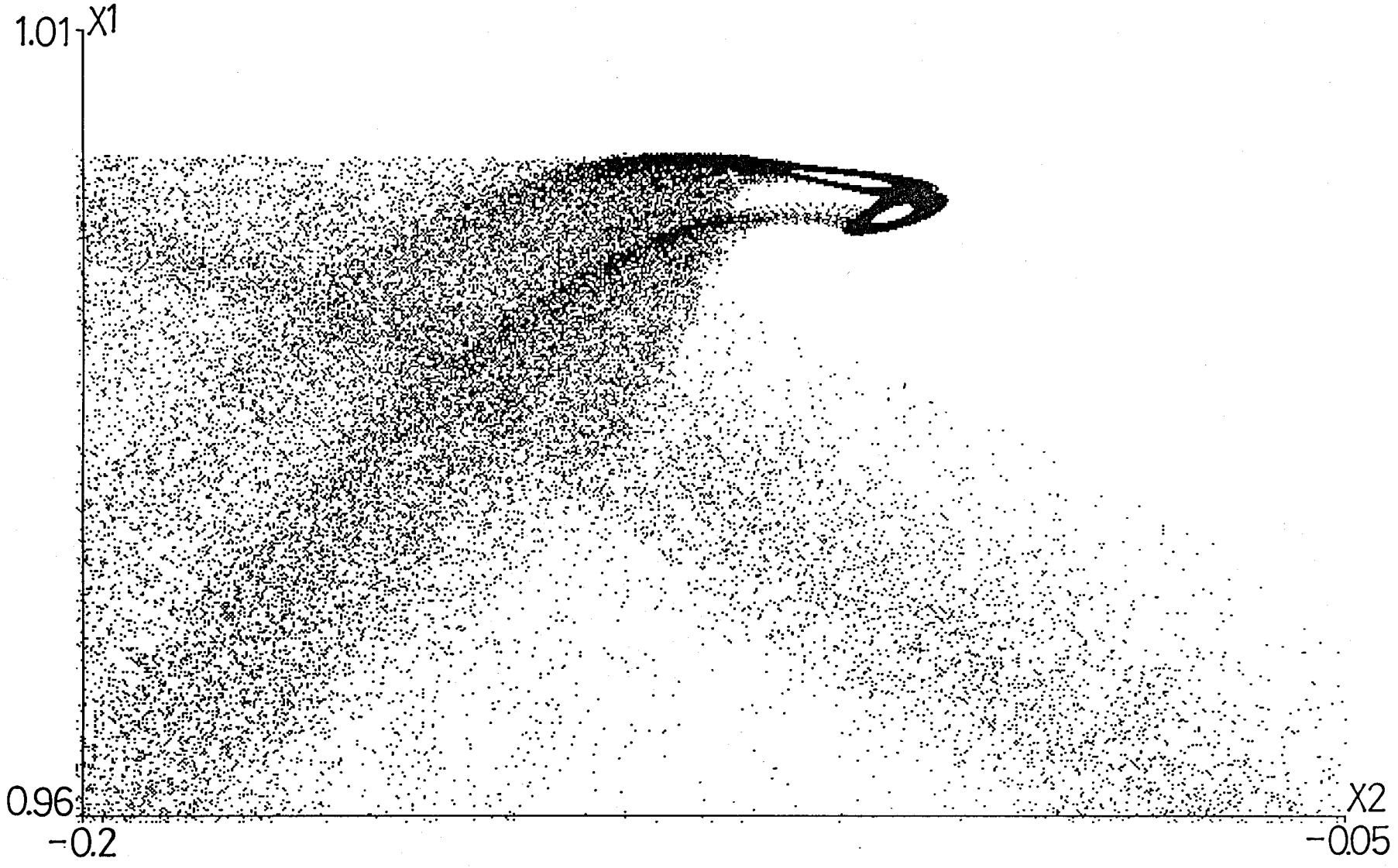

Fig. 3 (b)

Okuda & Tsuda

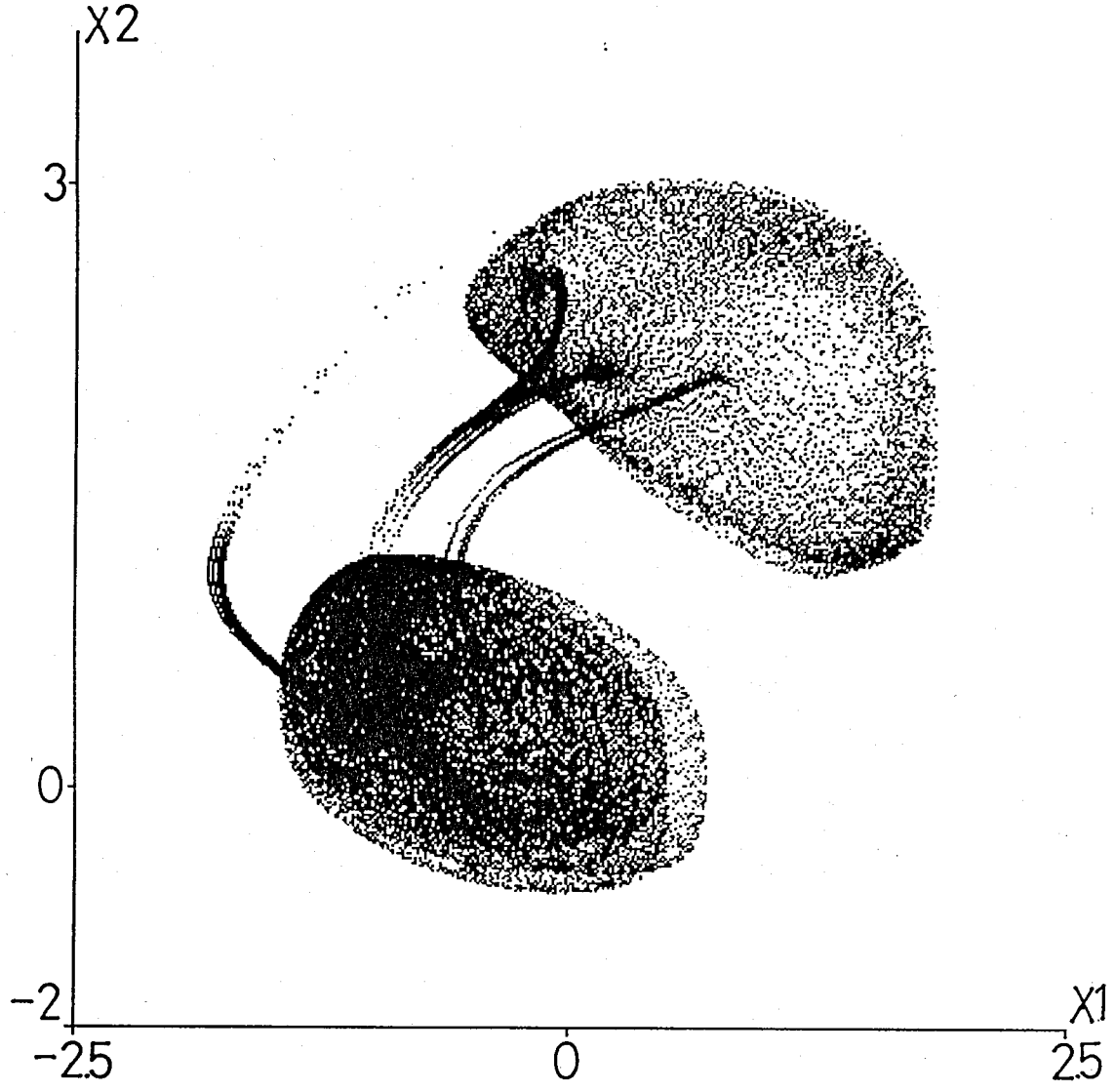

Fig. 4 (a)

Okada & Tsuda

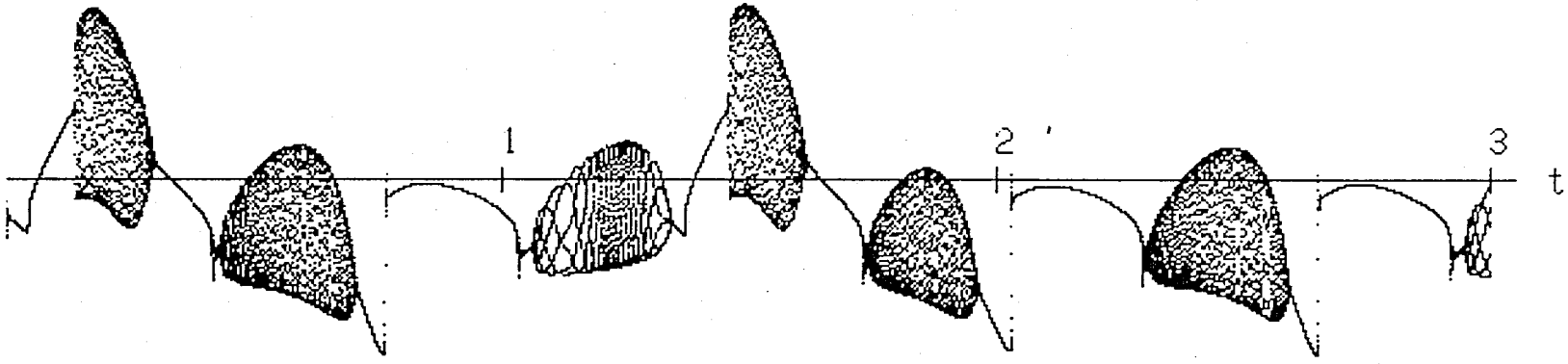

Fig. 4 (b)

Okuda & Tsuda

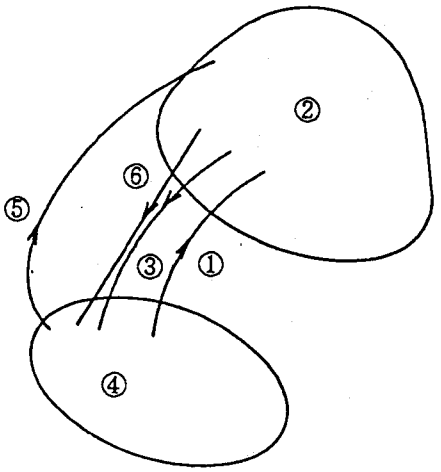

Fig. 5

Okuda & Tsuda

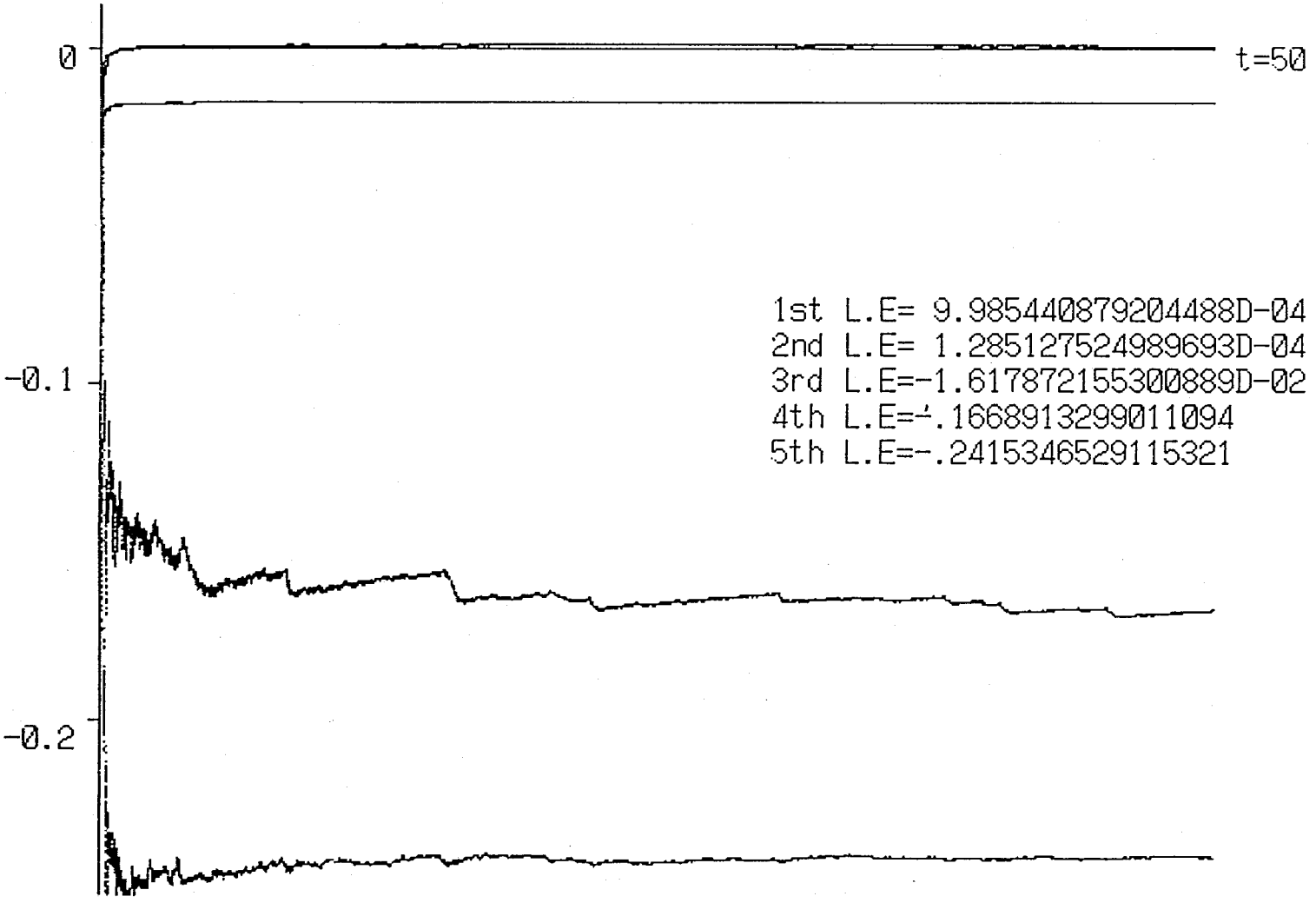

Fig. 6

©Ikeda & Tsuda

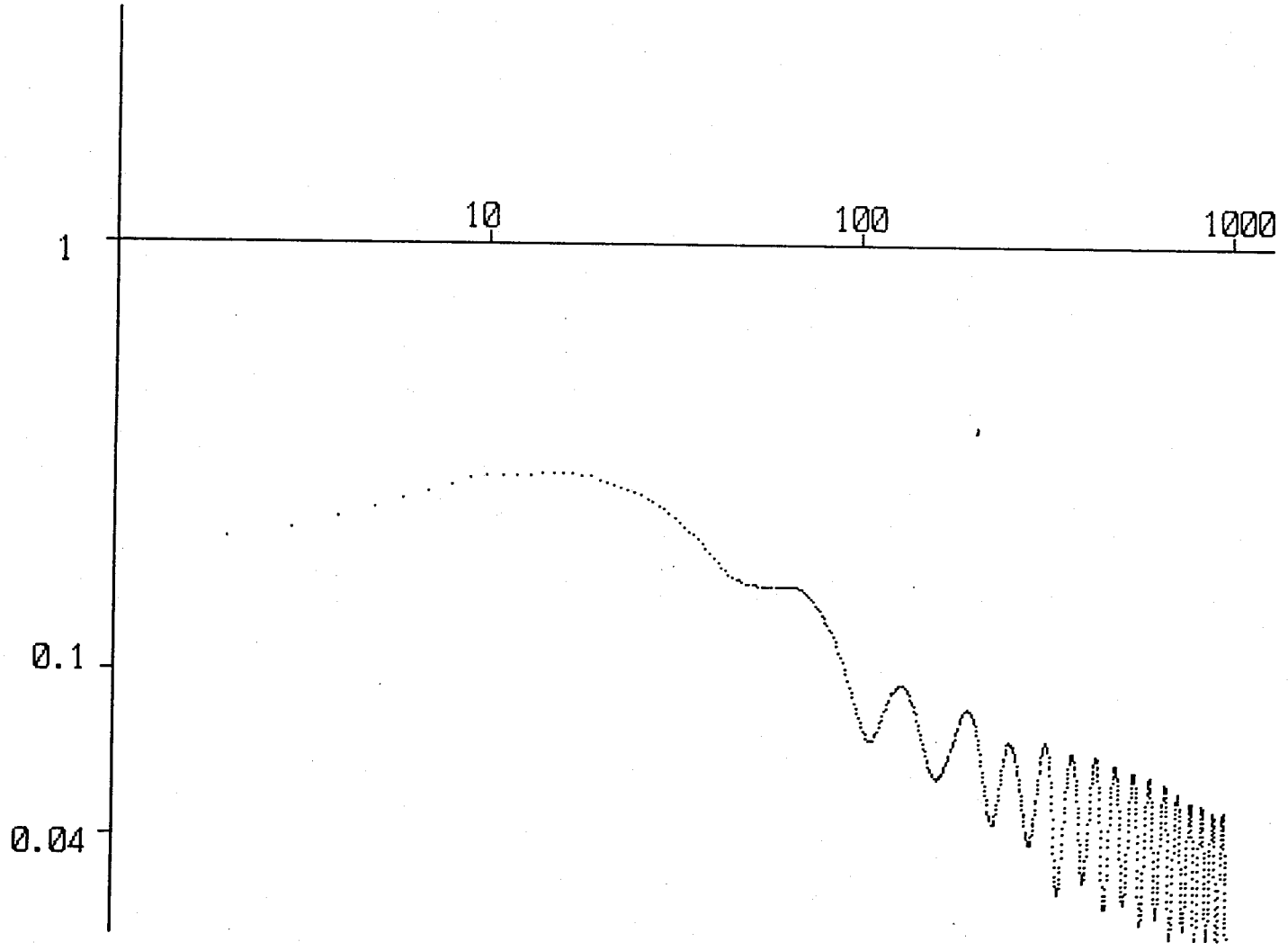

Fig. 7

©Ruda & Tsuda

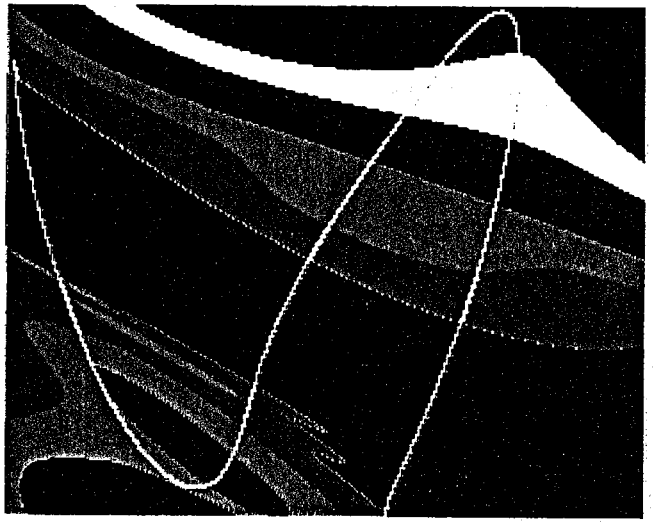

Fig.8 (a)

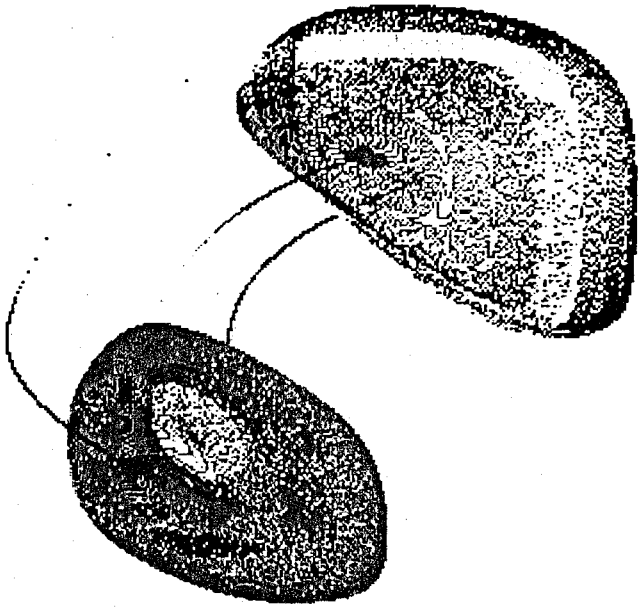

Fig.8 (b)

Okuda & Tsuda

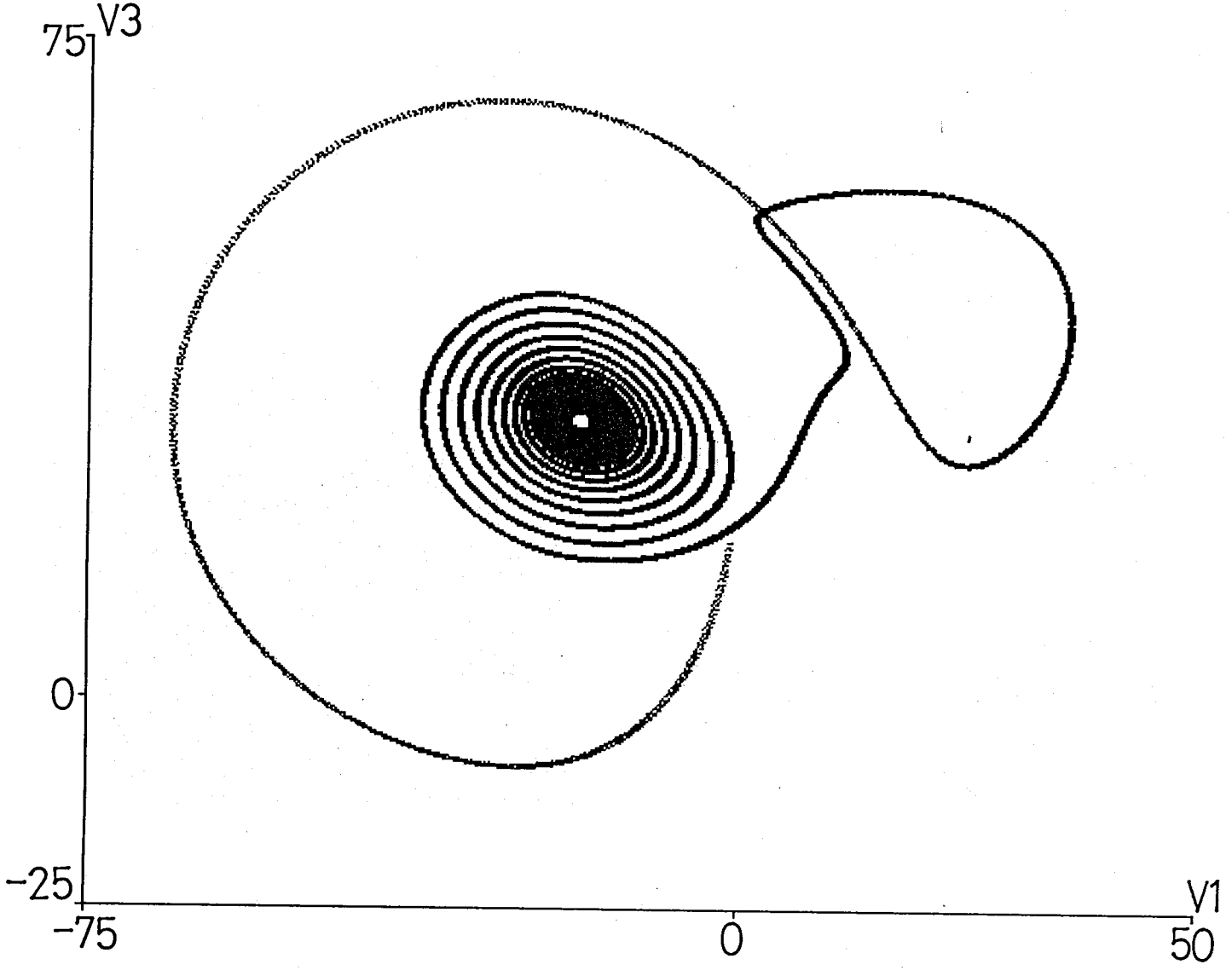

Fig. 9 (a)

Okuda & Tsuda

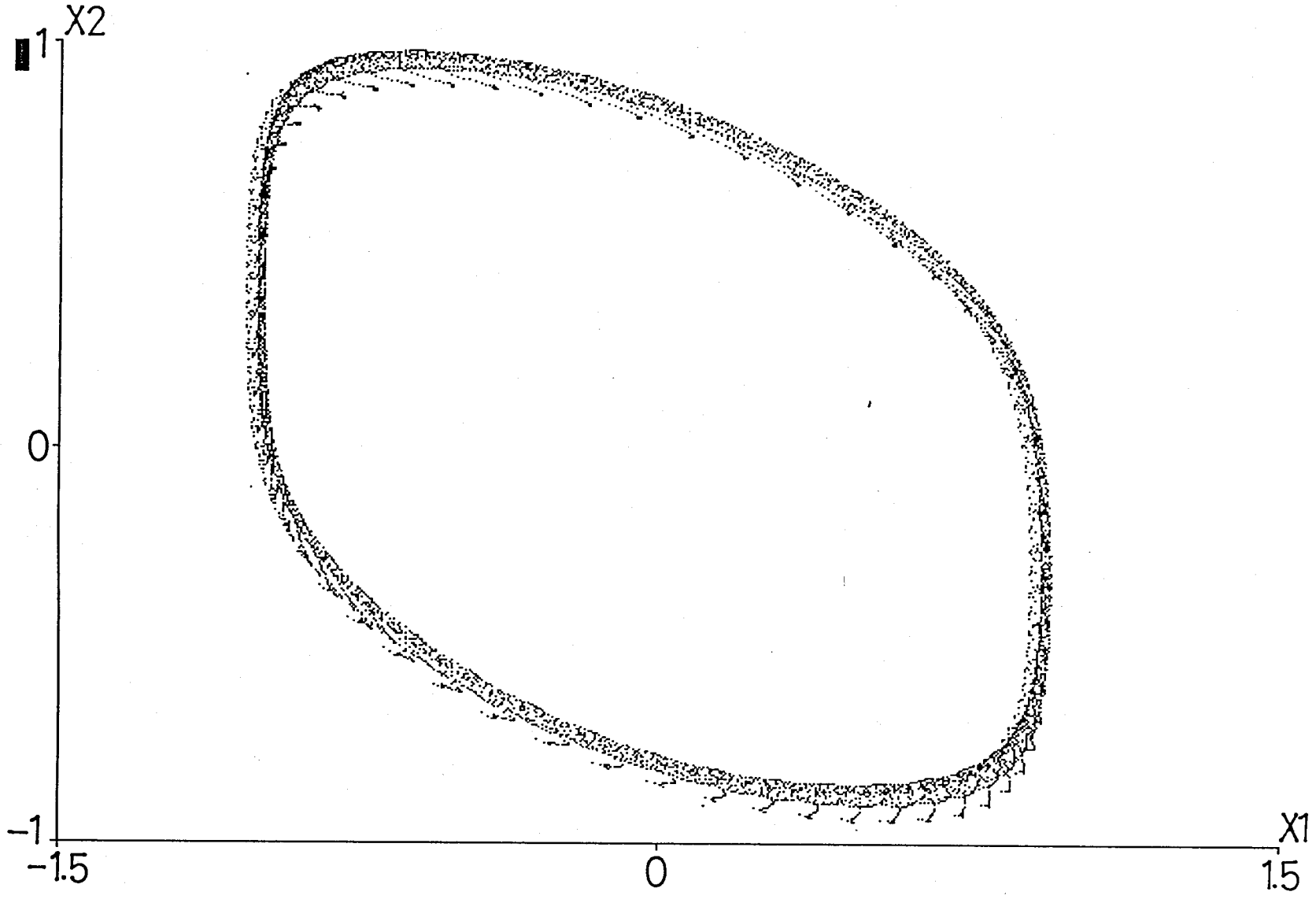

Fig. 9 (b)

Okuda & Tsuda

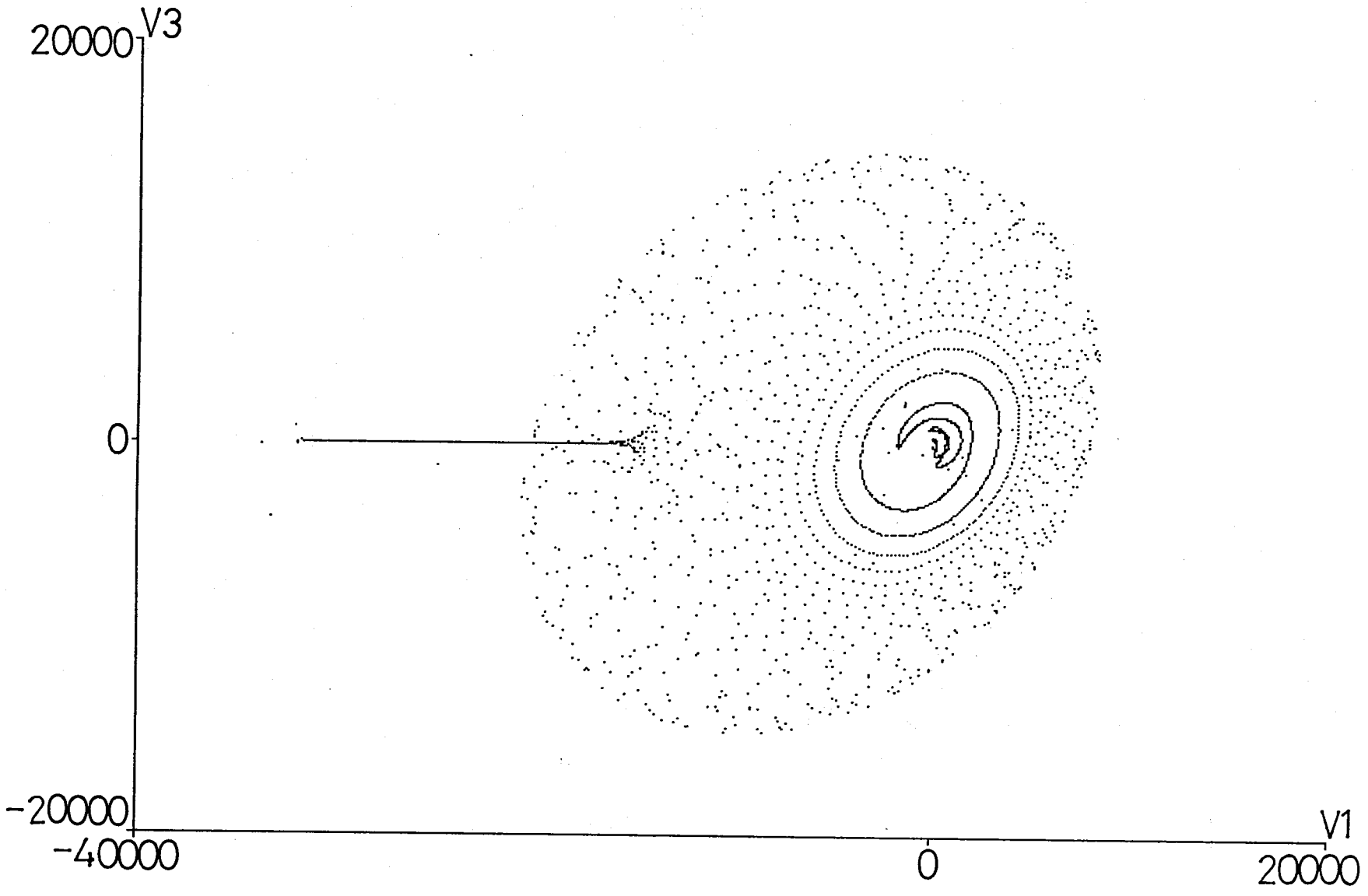

Fig. 10 (a)

Okuda & Tsuda

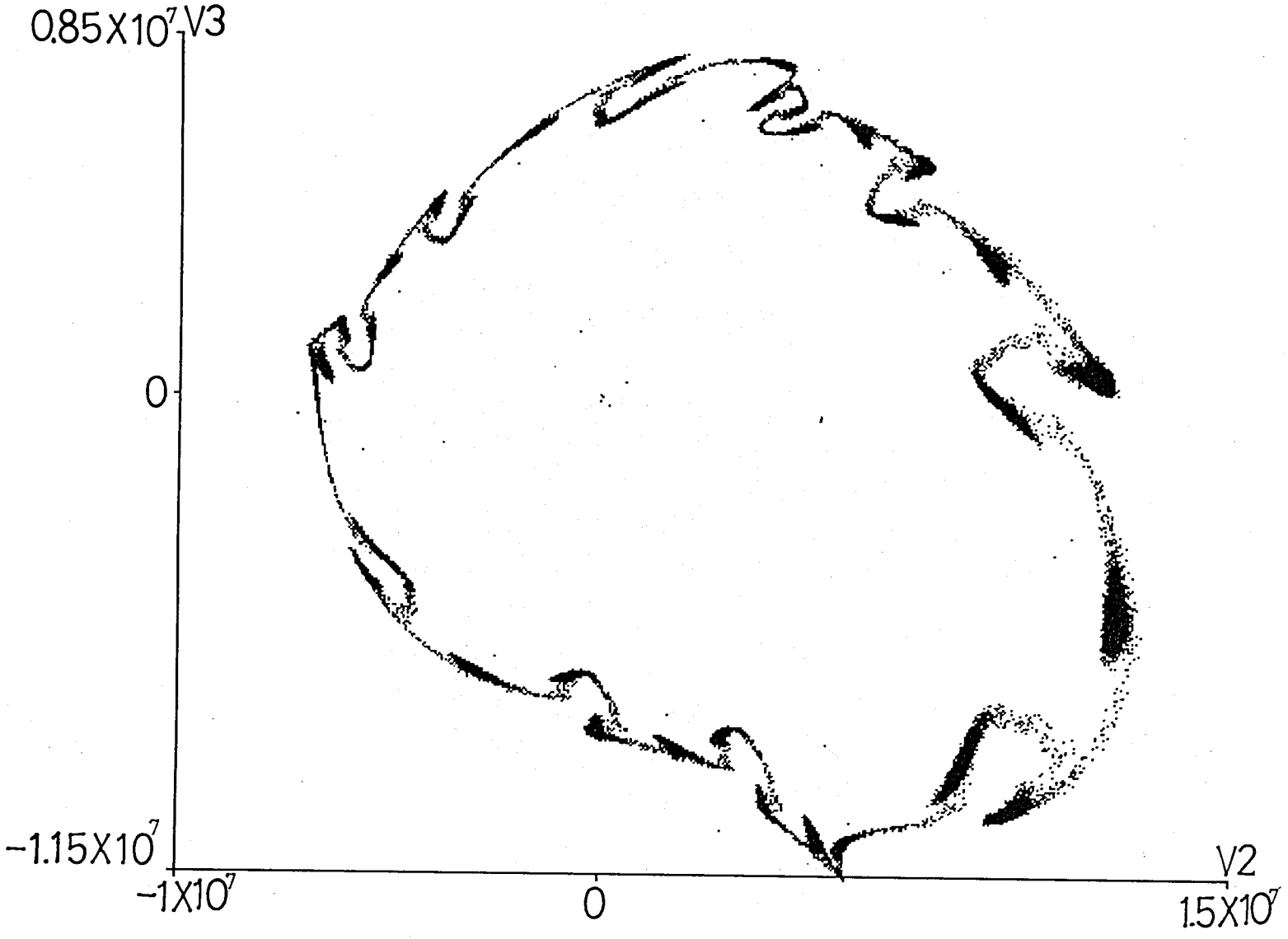

Fig. 10 (b)

Okuda & Tsuda

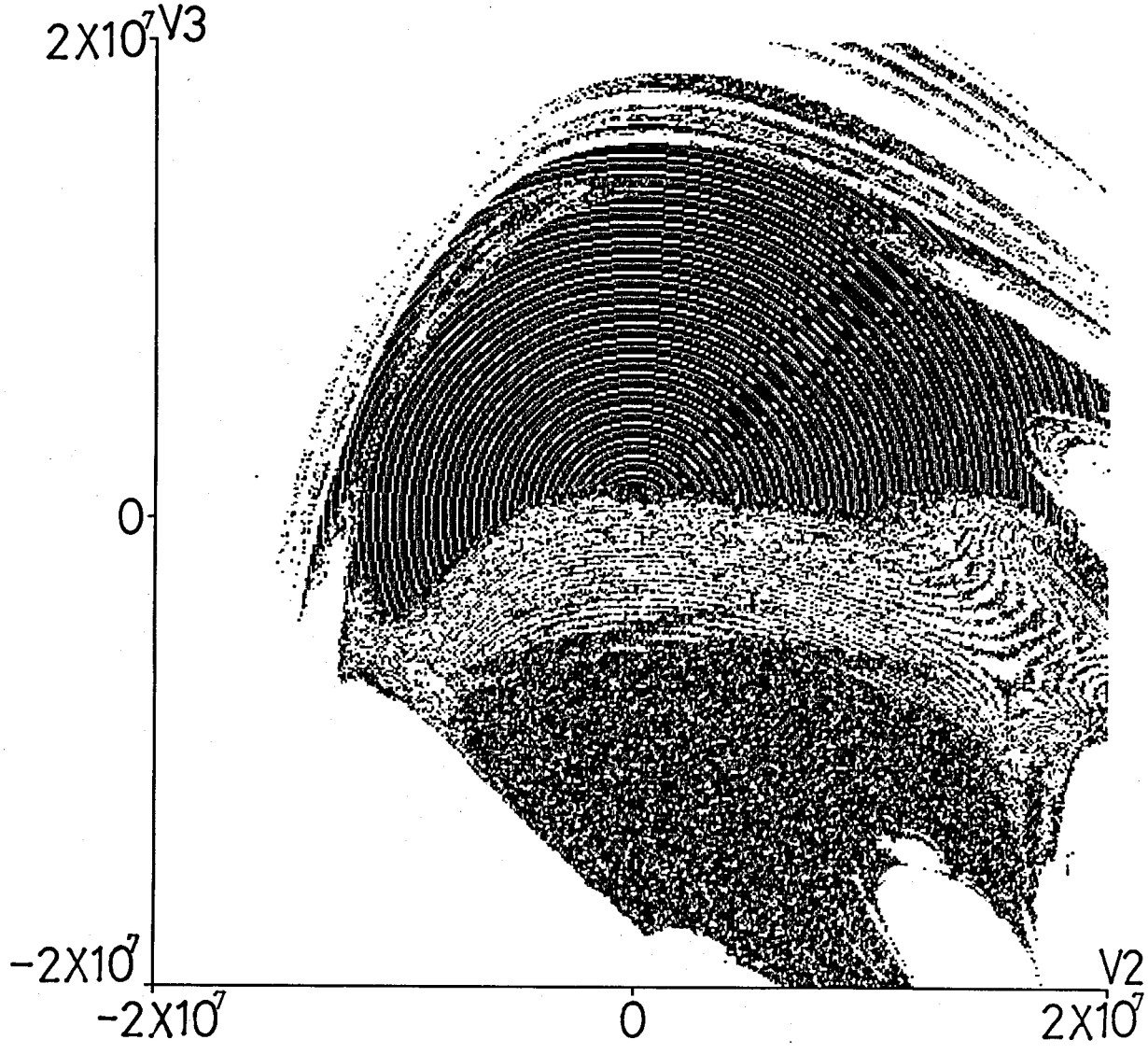

Fig. 11

Okuda & Tsuda

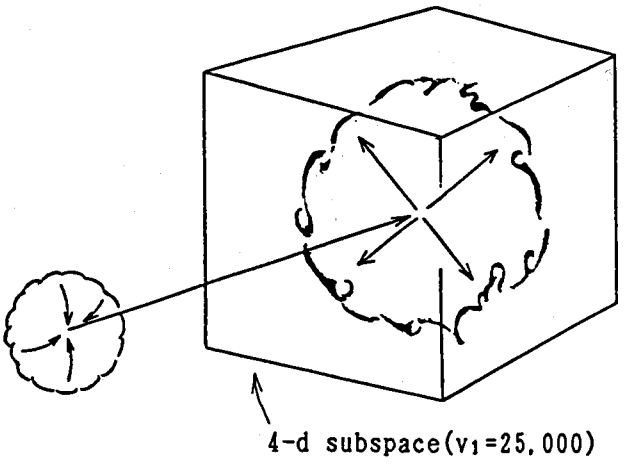

Fig. 12(a)

Okuda & Tsuda

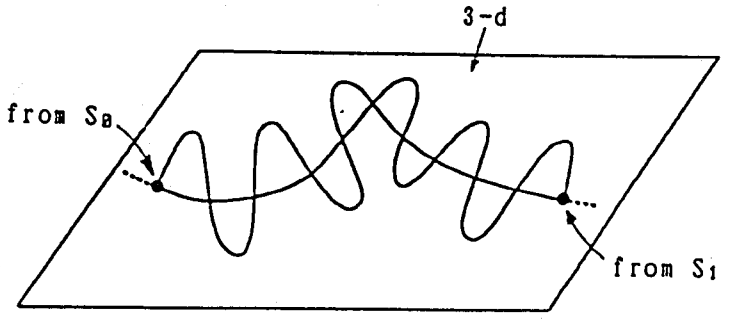

Fig. 12(b) Okuda & Tsuda

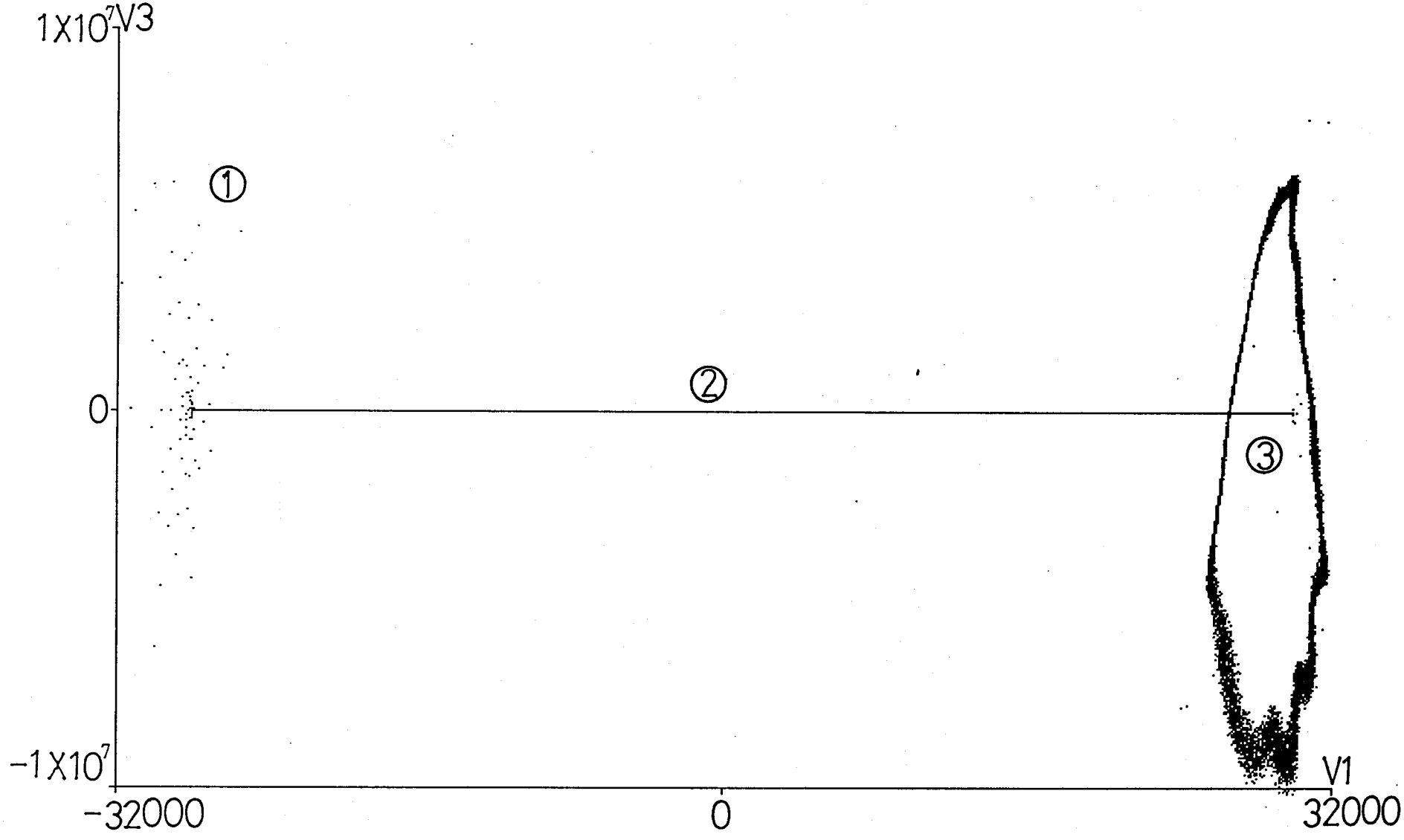

Fig.13

Okuda & Tsuda

Fig. 14

Okuda
& Tsuda